

## ON THE ANALYSIS STRAIN MEASUREMENTS NEAR THE CRACK TIP

José Celio Dias, [jcelio@unifei.edu.br](mailto:jcelio@unifei.edu.br)

Ricardo Dutra Mendes, [rdm@unifei.edu.br](mailto:rdm@unifei.edu.br)

Federal University of Itajubá - UNIFEI, Institute of Mechanical Engineering - IEM, Prof. José Rodrigues Seabra Campus, 1303 BPS Av., Pinheirinho District, ZIP code 37500-903, Box-Postal 50, Itajubá, Minas Gerais, Brazil.

**Abstract.** The goal of this work is obtaining a better knowledge about the Specific Strain field in some points along the prospective crack path, been this crack from a normal traction, of a half-finite plate with a lateral crack of a circumference arc subdued to a uniform remote tensile stress. In these geometric and requested conditions, the ligament region is subdued to a force and bending apply, both concentrated in the middle point of the ligament. With the specific strain measurements obtained by experimental analysis using strain gages, the intensity stress factor  $K_I$  can be determined. Due to the effect of the hysteresis, by the conditions of loading and unloading in the strain gages, it is convenient to elaborate a theoretical study, for example, by Finite Elements Method (FEM) analysis. This procedure seems to be satisfactory, allowing the theoretical-experimental analysis. At this point, the calculation of  $K_I$  is obtained using FEM, and the technique of specific strains and extrapolation of values around the crack tip. The results are compared with others, obtained using different methods, like nodal forces.

**Keywords:** half-finite plate, lateral crack, finite elements, strain gage, accuracy of strain.

### 1. INTRODUCTION

The plasticity-induced crack closure phenomenon is the leading mechanism which controls the main effects on fatigue crack growth, such stress ratio and load interaction effects, in metallic materials. Since the pioneering work of Elber (1970), it has been recognized that the effective driving force for crack growth might be better characterized by using the effective stress intensity factor range. A range of experimental techniques have been used moiré interferometer methods like Gray and MacKenzie (1990) or Fellows and Nowell (2004); the ultrasonic method (Rokhlin and Kim, 2003); the potential drop technique (Ghajar, 2004); acoustic emission technique (Lee *et al.*, 1986); the photoelasticity method (Pacey *et al.*, 2005) and synchrotron X-ray micro-tomography (Toda *et al.*, 2004). Other techniques used are analytical models such as that proposed by Budiansky and Hutchinson (1978), and Newman (1981). Many researchers have simulated plasticity-induced fatigue crack closure in 2D or 3D geometries using Finite elements method under plane strain (Fleck, 1986; Zhao *et al.*, 2004; Wang *et al.*, 2002; McClung *et al.*, 1991; Pommier, 2002; Lee and Song, 2005) or plane stress conditions by Zhao, and McClung *et al.* (1989a-b) and Solanki (2002). Also analytical model such as that proposed by Newman had been performed.

All techniques, whether experimental or theoretical require a definition of crack opening or closure. We wish to give a particular emphasis to the techniques used to access the crack opening stress in local compliance analysis. Local compliance measurements were used near the crack tip. This is the reason why strain gauges bonded were allocated at the specimen to measure the stress level,  $S_{op}$  (or  $S_{opening}$ ), at which a crack is fully opened at the crack tip during loading, and the stress level,  $S_{cl}$  (or  $S_{closure}$ ) at which closure starts at the crack tip. A partly non-linear record is obtained schematically as shown in figure 1, which may show hysteresis. It may also suggest that crack opening and crack closure do not start at the exactly same stress level (Schijve, 2001). These stress levels are the transition points between the non-linear part and linear of the record. It is not always fully clear at which stress level this occurs. Sometimes, the transition is better observed during unloading than during loading while the latest one is theoretical of greater interest.

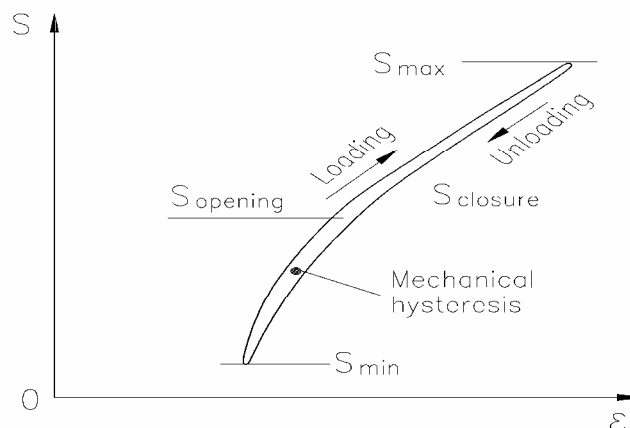


Figure 1. Hysteresis of crack opening and crack closure.

In the analysis of local compliance measurements the problem comprises:

- The approach initially consists in the acquisition of a stress-strain ( $S$ - $\epsilon$ ) diagram.
- The sensitivity of the measurement in terms of the distance between the strain gauge and the crack tip, it is, the field of applicability of *Local Compliance* method.

The purpose of this study is to employ the finite elements method to verify the accuracy of the local compliance measurements, using ANSYS® program. Numerical examples are given for the elucidation the procedure employed, thus allowing the theoretical-experimental analysis. Currently, experimental attempts focuses in obtain the specific strain with strain gauges device's help, that may be located around the crack tip.

## 2. BASICS CONCEPTS

Between the different calculation procedures of stress intensity factor through the approach of finite elements, we may mention: *Nodal Forces* method and *Specific Strain* method. Hence, the last method cited shows advantages in the theoretical-experimental analysis.

### 2.1 Experimental procedure

The procedure consists in using strain gauges bonded near the crack tip as showed in figure 2. The value of the specific strain is relatively easy to be obtained through experimental analysis of tension/deformation. A pair of strain gauges can be positioned adequately, as shown in the example, oriented in the direction of the main axes,  $x'$  e  $y'$ . Thus, in these conditions, the angles  $\alpha$  e  $\alpha + 90^\circ$  define the main directions. Hence, the tensions and main deformations are evaluated by a simple data acquisition system.

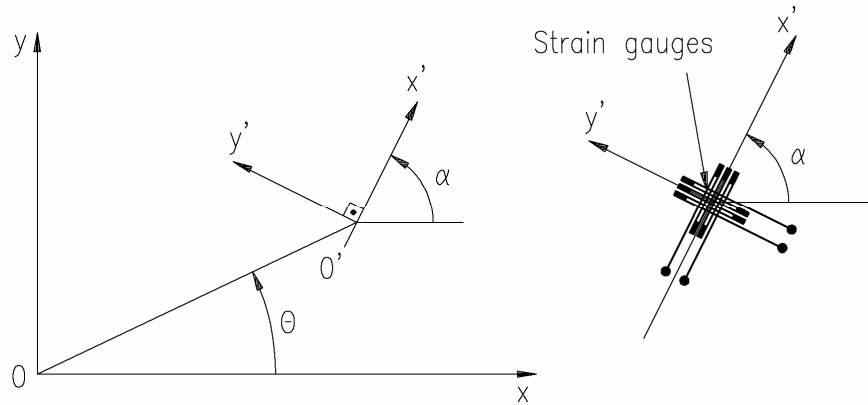


Figure 2. Coordinate system definition.

### 2.2 Specific strain method

The strain field can be described by the follow (Dally and Riley, 1991):

$$\epsilon_{ij} = A_1 f_{ij}(\theta) r^{-1/2} + A_2 g_{ij}(\theta) r^0 + A_3 h_{ij}(\theta) r^{1/2} + \dots \quad (1)$$

Where  $r$  and  $\theta$  are the radio and the angle, measured in the crack tip, in that order. Every  $A_i$  ( $i=1,2,\dots$ ) are constants in the equation.  $f_{ij}(\theta)$ ,  $g_{ij}(\theta)$  and  $h_{ij}(\theta)$  are dimensionless functions of  $\theta$  and  $\alpha$ . The variable  $\alpha$  is the positioning angle of the strain gauges projected in the axis  $x$ . The value of  $A_1$  is given by equation  $A_1 = K_I / (2\pi)^{1/2}$ .

Since we evaluated the specific strains  $\epsilon_{x'x'}$ , the following equation will determine the constants  $A_i$  (Dally and Riley, 1991) by the application of the conditions conveniently chosen.

$$2G\epsilon_{x'x'} = \frac{A_1}{\sqrt{r}} \left[ k \cos \frac{\theta}{2} - \frac{1}{2} \text{sen}\theta \text{sen} \frac{3\theta}{2} \cos 2\alpha + \frac{1}{2} \text{sen}\theta \cos \frac{3\theta}{2} \text{sen} 2\alpha \right] \quad (2)$$

$$+ A_2 (k + \cos 2\alpha) + A_3 \sqrt{r} \cos \frac{\theta}{2} \left[ k + \text{sen}^2 \frac{\theta}{2} \cos 2\alpha - \frac{1}{2} \text{sen}\theta \text{sen} 2\alpha \right]$$

Where  $k = (1-\nu)/(1+\nu)$  and  $G = E/2(1+\nu)$ . In this equation,  $E$  is the Young's modulus and  $\nu$  is the Poisson's ratio. Given the conditions  $\theta = \alpha = 60^\circ$  and  $\nu = 0.333$ , it can be written in the following equation:

$$A_1 = 2E\varepsilon_{x'x'}\sqrt{\frac{r}{3}} \quad (3)$$

As commented before, the calculation of the stress intensity factor will be obtained by the finite elements method employing ANSYS® (quadrilateral element PLANE82), using in the technical of the specific strain and extrapolation of values around the crack tip. The results of the method may be compared with others, like *Nodal Forces* and analytic techniques.

### 2.3 Analytic method

Analytically, the stress intensity factor in a half-finite plate with a lateral crack of a circumference arc subdued to a uniform remote tensile stress, as planned in the figure 3(a), is described by the follow equation (Cherepanov, 1979):

$$K_I = \sqrt{\pi} \left[ \left( \frac{4\pi - 12}{\pi^2 - 8} \right) \left( \frac{P_\infty}{\sqrt{c}} \right) + \left( \frac{4\pi - 8}{\pi^2 - 8} \right) \left( \frac{M_\infty}{c\sqrt{c}} \right) \right] \quad (4)$$

The figure 3(b) shows the condition of loading in these geometric and requested conditions. The ligament region is subdued to a stress force  $P_\infty$  and bending torque  $M_\infty$ , both concentrated in the middle point of the ligament  $c$ . The lateral crack is from circumference arc with radius equal an  $R$  and a distance  $d$  from one of the plate faces.

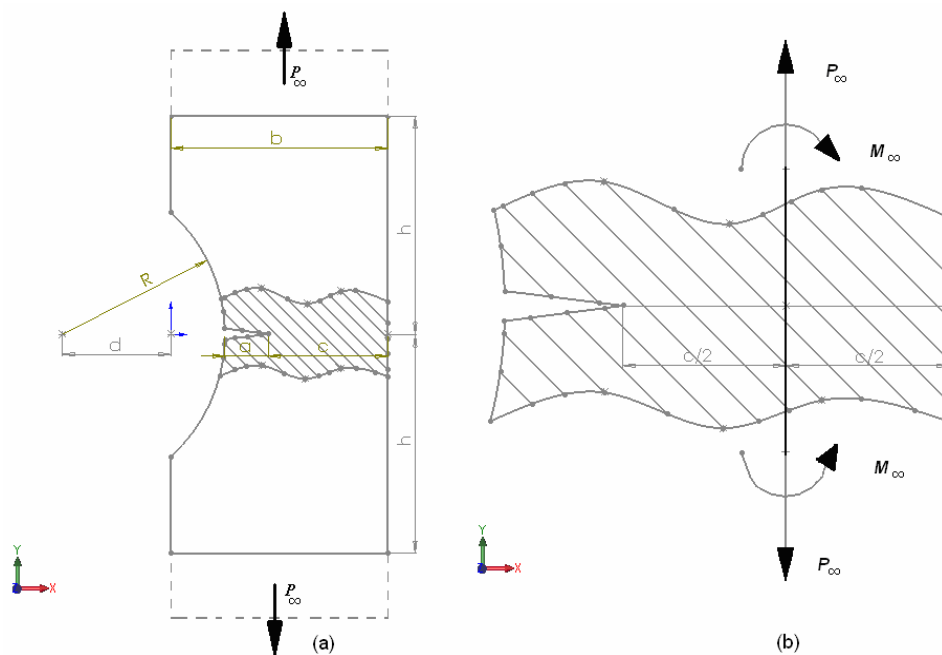


Figure 3. (a) half-finite plate with a lateral crack of a circumference arc, (b) tensile stress detail in the hatch region.

### 2.4 Nodal forces method

This calculation procedure consists in obtaining the nodal forces along the front of the crack in its plane. These forces can be evaluated by numerical methods, by the stress intensity factor obtained by the expression (Castro, 2006):

$$K_I = \sqrt{\frac{\pi}{2x_c}} \sum_{i=1}^n F_{y,i} \quad (5)$$

Where  $F_y$  is the nodal force,  $x_c$  is the abscissa for the  $i$ th position for the respective nodal force.

### 3. RESULTS ANALYSIS

The analysis consider a half-finite plate with a lateral crack of a circumference arc subdued to a  $25MPa$  of uniform remote tensile stress as shown in the figure 4. The material properties used were aluminum, with young's modulus of  $70 GPa$  and Poisson's ratio  $\nu = 0,333$ . The dimensions of the plate one are  $b = 200mm$ ,  $h = 200mm$  and  $d = 100mm$ . As in the previous paragraph, the specimen has been subjected to a monotonic load/thickness of  $5MN/m$  correspondent to a maximum stress level.

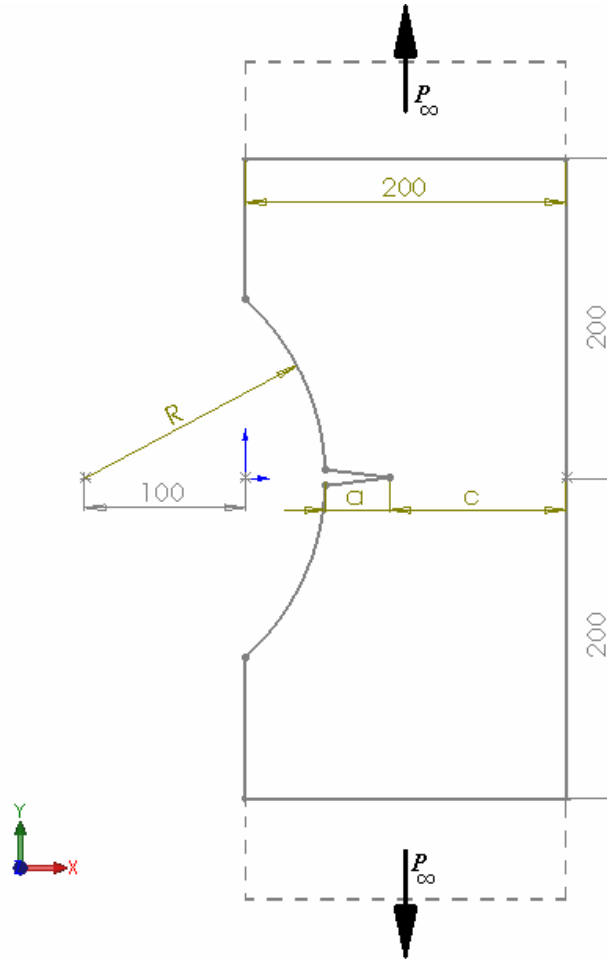


Figure 4. Aluminum plate with lateral crack under loading.

#### 3.1. Calculation procedure

The figure 5 shows the  $K_I$  factor as a function of the distance  $r$  for  $\theta = \alpha = 60^\circ$ . In this example, the dimensions used were  $R=150mm$  and  $a=10mm$ . The technique consists in determining the specific strains that leads to the evaluation of the constant  $A_1$ ,  $A_2$  and  $A_3$ . The first constant allows determining the stress intensity factor; therefore the others are not important at the moment. The calculation of the stress intensity factor is obtained through the technical of specific strains and extrapolation of values around the crack tip. The expression of this straight line is given by lineal regression in the form:  $K_I = 0.0187r + 19.355$ . Hence, we arrive to the equation  $K_I = 19.355MPa\sqrt{m}$ . Thus, the analytic value found is  $19.572 MPa\sqrt{m}$ , with error = 1.1%.

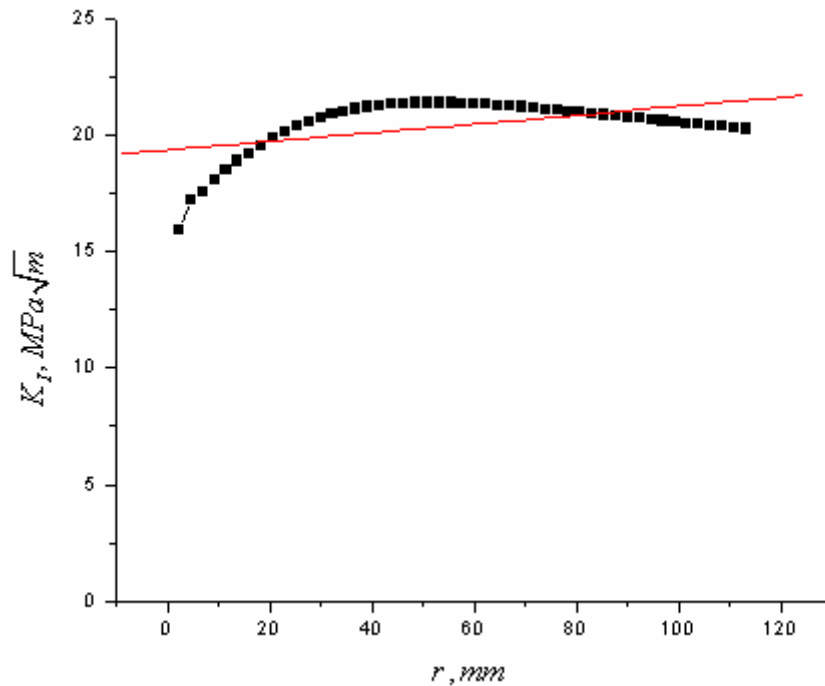


Figure 5.  $K_I$  as a function of the  $r$ .

### 3.2. Analytical/numerical methods

The figures 6(a-d) show the behavior of the  $K_I$  factor as a function of the crack length, for different values of  $R$ . We would like to say that in an obtainment of these graphics, were omitted its steps which, in other opportunity will be showed. As may be seen in these graphics the divergence between the analytic method and the *Specific Strain* method is very small, it yields errors less than 5%. The difference between the values obtained by the *Specific Stains* method and the *Nodal Forces* method are convergent for values of  $R$  less than 150mm. For higher values, occurs an accentuated discrepancy between the values, especially in small crack lengths. One way to improve the *Nodal Forces* method analyze results would be refining the finite elements mesh, located around the crack tip.

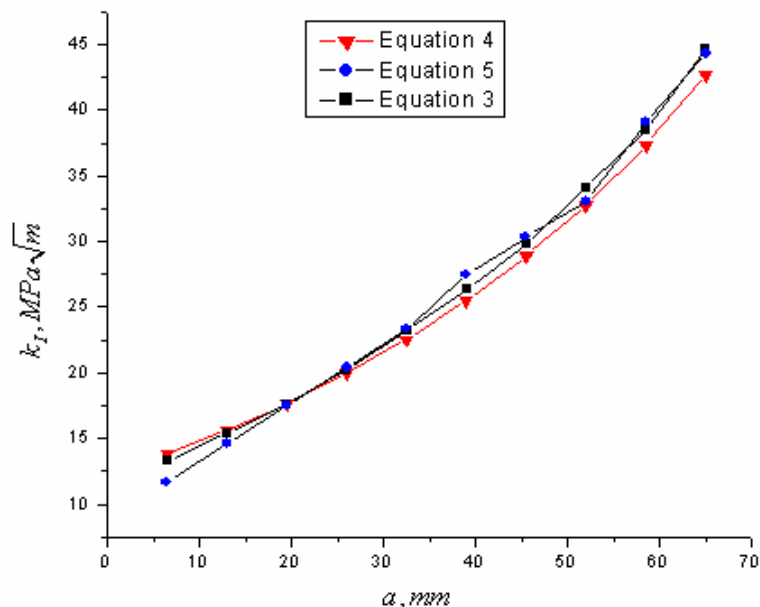


Figure 6a. Comparison between analytical and numerical results for  $R=135\text{ mm}$ .

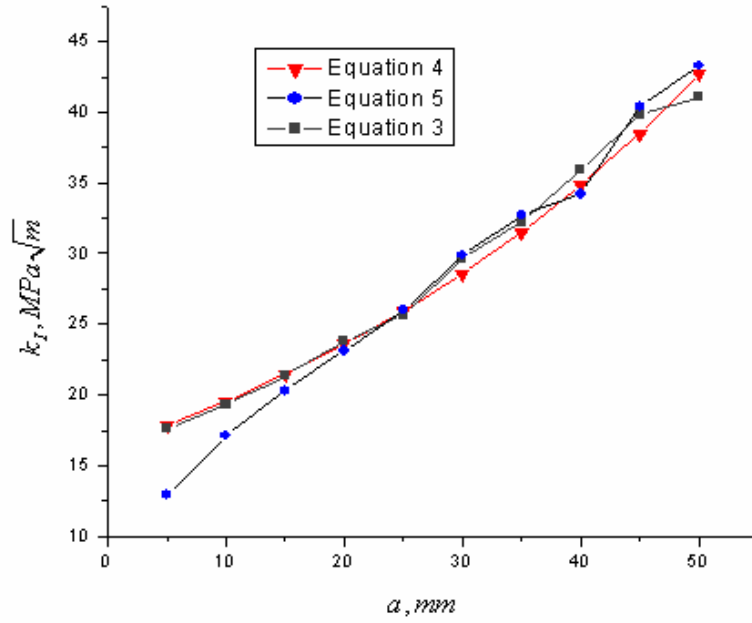


Figure 6b. Comparison between analytical and numerical results for  $R=150\text{ mm}$ .

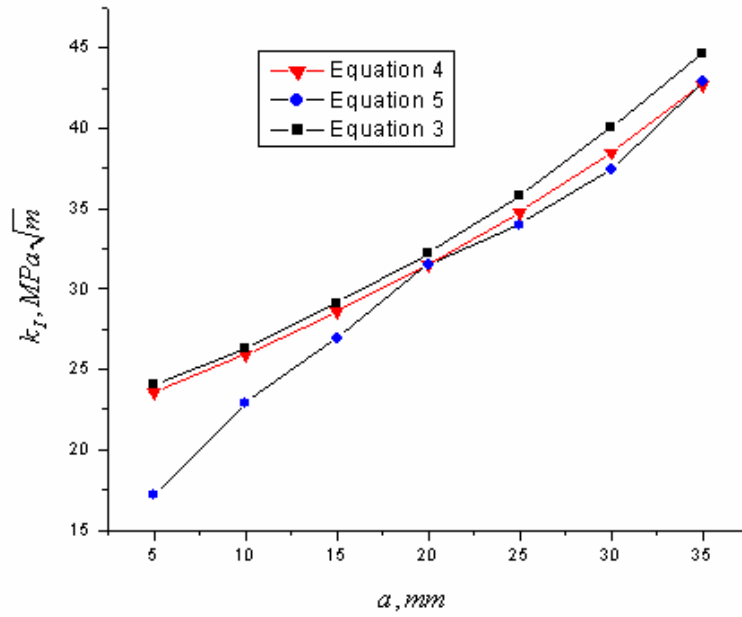


Figure 6c. Comparison between analytical and numerical results for  $R=165\text{ mm}$ .

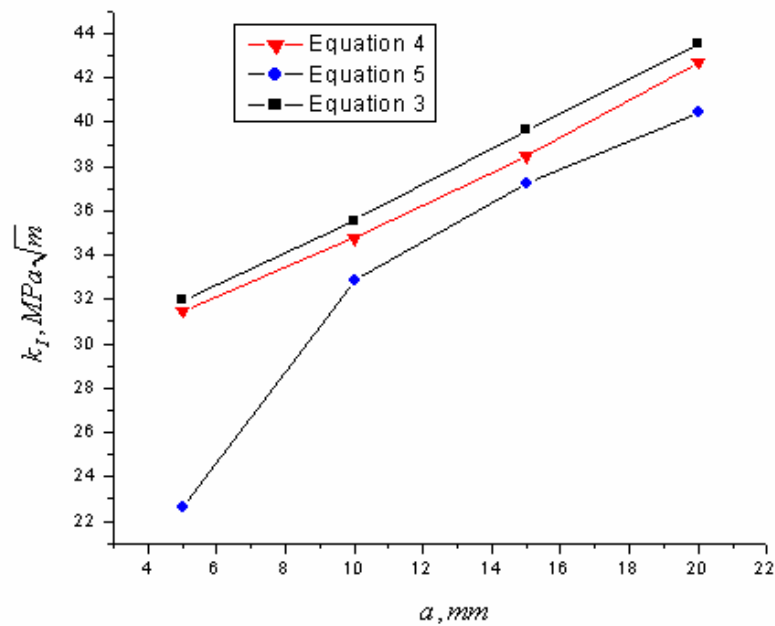


Figure 6d. Comparison between analytical and numerical results for  $R=180 \text{ mm}$ .

### 3.3. Theoretical-experimental analysis

Currently, experimental attempts focus on obtaining the specific strain with strain gauge devices, that may be located around the crack tip. A pair of sensors is positioned on  $\theta = \alpha = 60^\circ$  with different values of  $r$ . Also they are positioned along the front part of the crack at its plane in  $\theta = 0^\circ$  and  $\alpha = 90^\circ$ . A data acquisition system channels/SPIDER8 with 8 input channels may be used, and the information is carried aiming a confrontation between the results. The procedure allows a theoretical/experimental analysis that determines the stress intensity factors in the combined loading ways *III*. It is, these ways refer to normal traction crack and shear crack on the plane. Then, the procedure aims an analysis of the structural integrity of mechanical elements and equipments.

## 4. CONCLUSIONS

It was approached by the use of the specific strain method the concept of local compliance. The procedure allows a theoretical analysis through the finite elements method. Some observations and conclusions are presented below.

The theoretical results by the analytic approach compared with the specific strain did not exceed an error of 5%. The procedure allows a theoretical/experimental analysis with strain gauges with base size within the range of 2 to 3mm, and the errors we found attend the experimental requirements.

The strain approach allows investigating stress intensity factors on combined loading ways *III*.

The obtained results apply for the maximum stress condition. However, the *Specific Strain* method, utilize the concept of local compliance. Thus, it is allowed to find recorded data for evaluate the stress's  $S_{opening}$  and  $S_{closure}$ .

The procedure of the experience shows that measurements close to the crack tip are better defined records than measurements taken at a distance from the crack tip. It is also foregone that strain gage measurements give more relevant information than displacement measurements by clip gages.

At the experimental results, their will be detailed and showed briefly in other an opportunity.

## 5. ACKNOWLEDGEMENTS

The authors would like to thank CNPq (Conselho Nacional de Pesquisa) by the support granted.

## 6. REFERENCES

- Elber W., 1970, "Fatigue crack closure under cyclic tension", Engng Fract Mech, Vol. 2, pp. 37-44.
- Gray TGF, MacKenzie PM., 1990, "Fatigue crack closure investigation using Moiré' interferometry", Int J Fatigue, Vol. 12, pp. 417-23.

- Fellows LJ, Nowell D., 2004, "Crack closure measurements using Moire' interferometry with photoresist gratings" *Int J Fatigue*, Vol. 26, pp.1075–82.
- Rokhlin SI, Kim J-Y., 2003 "In situ ultrasonic measurement of crack closure" *Int J Fatigue*, Vol.25, pp. 51–8.
- Ghajar R., 2004 "An alternative method for crack interaction in NDE of multiple cracks by means of potential drop technique", *NDT&E Int*, Vol. 37, pp. 539–44.
- Lee CS, Livne T, Gerberich WW., 1986, "The acoustic emission measurement of cleavage initiation near the ductile brittle transition temperature in steel" *Scripta Metall* , Vol. 23, pp. 1137–40.
- Pacey MN, James MN, Patterson EA., 2005, "A new photoelastic model for studying fatigue crack closure" *Exp Mech*", Vol. 45, pp. 42–52.
- Toda H, Sinclair I, Buffiaere J-Y, Maire E, Khor KH, Gregson P, Kobayashi T., 2004, "A 3D measurement procedure for internal local crack driving forces via synchrotron X-ray microtomography", *Acta Mater*, Vol. 52, pp. 1305–17.
- Budiansky B, Hutchinson JW., 1978, "Analysis of closure in fatigue crack growth" *J Appl Mech – Trans ASME*, Vol. 45, pp.267–76.
- Newman Jr JC., 1981, "A crack-closure model for predicting fatigue crack growth under aircraft spectrum loading", *ASTM STP*, 748, pp. 53–84
- Fleck NA., 1986, "Finite element analysis of plasticity-induced crack closure under plane strain conditions", *Engng Fract Mech*, Vol. 25, pp. 441–9.
- Zhao LG, Tong J, Bryne J., 2004, "The evolution of stress strain fields near a fatigue crack tip and plasticity-induced crack closure revisited" *Fatigue Fract Engng Mater Struct*, Vol. 27, pp.19–29.
- Wang CH, Rose LRF, Newman Jr JC., 2002, "Closure of plane strain-cracks under large-scale yielding conditions.", *Fatigue Fract Engng Mater Struct*, Vol. 25, pp.127–39.
- McClung RC, Thacker BH, Roy S., 1991, "Finite element visualization of fatigue crack closure in plane stress and plane strain", *Int J Fract*, Vol. 50, pp. 27–49.
- Pommier S.,2002, "Plane strain crack closure cyclic hardening" *Engng Fract Mech*, Vol. 69, pp.25–44.
- Lee HJ, Song JH., 2005, "Finite-element analysis of fatigue crack closure under plane strain conditions: stabilization behavior and mesh size effect", *Fatigue Fract Engng Mater Struct*, Vol. 28, pp. 333–42.
- McClung RC, Sehitoglu H., 1989, "On the finite element analysis of fatigue crack closure – 1 Basic modeling issues", *Engng Fract Mech*, Vol. 33, pp. 237–52.
- McClung RC, Sehitoglu H., 1989, "On the finite element analysis of fatigue crack closure – 2 Numerical results", *Engng Fract Mech*, Vol. 33, pp. 253–72.
- Solanki KN., 2002, "Two and three-dimensional finite element analysis of plasticity-induced fatigue crack closure – a comprehensive parametric study" MSc thesis, Mississippi State University.
- Schijve JAAP, 2001, "Fatigue of Structures and Materials", Kluwer Academic Publishers, 360 p.
- Dally JW and Rilely WF, 1991, "Experimental Stress Analysis", McGraw Hill, 329 p.
- Cherepanov GP, 1979, "Mechanics of Brittle Fracture", McGraw Hill, 303 p.
- Personal home page, Professor Paulo M S Tavares de Castro. 2 Nov. 2006  
<[http://paginas.fe.up.pt/~ptcastro/Mec\\_Fract\\_6\\_4\\_6\\_force\\_method-1.ppt](http://paginas.fe.up.pt/~ptcastro/Mec_Fract_6_4_6_force_method-1.ppt)>

## 7. RESPONSIBILITY NOTICE

The authors are the only responsible for the printed material included in this paper.